

Nucleate boiling on the superhydrophilic surface with a small water impingement jet [☆]

Yu-hao Qiu, Zhen-hua Liu ^{*}

School of Mechanical Engineering, Shanghai Jiaotong University, Shanghai 200030, China

Received 20 October 2006; received in revised form 8 May 2007

Available online 24 October 2007

Abstract

In this study, the coating process on the copper surface with titanium dioxide (TiO₂) has been introduced. The coated surface exhibits extremely high affinity for water and the solid–liquid contact angle decreases nearly to zero by exposing the surface to ultra-violet light. This superhydrophilic characteristic was applied to nucleate boiling heat transfer of water jet impingement on a flat heated plate. By making use of this special heat transfer surface, the nucleate boiling heat transfer and the critical heat flux (CHF) of a bar water jet impingement on a large flat superhydrophilic surface was experimentally investigated. The experimental data were measured in a steady state. The purified water was employed as the working liquid. Three main influencing factors, i.e., subcooling, impact velocity and the surface coating condition, were changed and their effects on the nucleate boiling heat transfer and the CHF were investigated. The empirical correlations were obtained for predicting the CHF of steady boiling for a small round water jet impingement on a large flat superhydrophilic surface. The experimental results show that the CHF on the superhydrophilic surface is about 30% higher than that on conventional copper surface by decreasing the solid–liquid contact angle.

© 2007 Elsevier Ltd. All rights reserved.

Keywords: Boiling; CHF; Jet; Superhydrophilic surface

1. Introduction

Titanium dioxide (TiO₂), one of the photo catalysts, has recently come into the spotlight because of its very attractive nature. One of its marvelous natures, which was discovered quite recently by researchers, is the superhydrophilicity [1]. When the surface coated with TiO₂ is irradiated by ultra-violet light, the solid–liquid contact angle for water decreases with time and finally reaches almost zero. This nature has various practical applications in the heat transfer field. By making use of the superhydrophilic heat transfer surface, the heat transfer characteristics of liquid–vapor phase change phenomena like boiling can be enhanced by ultra-violet irradiation [2,3].

The mechanism of super hydrophilicity is divided into three processes [1]. In the first process, when the surface of TiO₂ is irradiated by ultra-violet light, a pair of electron and hole is created by excitation. $h\nu \rightarrow e^- + h^+$. In case of usual photocatalytic reaction, this electron-hole pair reacts with oxygen or water that are adhering to the surface and then produce superoxide radical anions ($\cdot O_2^-$) and hydroxyl radical ($\cdot OH$). However, in case of photo-induced superhydrophilicity, TiO₂ crystal surface itself is reduced and oxygen vacancy is created. $e^- + Ti^{4+} \rightarrow Ti^{3+}$, $4h^+ + 2O^{2-} \rightarrow O_2$. Ti^{3+} is immediately oxidized by oxygen in the air and, on the other hand, oxygen vacancy bonds water molecule in the air. Finally, hydroxyl group (OH) is created on the surface and this acts as chemisorbed water layer.

Water jet cooling has been widely used in the iron or steel industry, nuclear power processes and many micro-electronic devices manufacturing and thermal management processes. For liquid boiling jet impingement on the hot plate, the assessment of the CHF is very important to

[☆] This paper was published in the 13th International Conference of Heat and Mass Transfer with the paper No. 2251.

^{*} Corresponding author. Tel./fax: +86 21 34206568.

E-mail address: liuzhenh@sjtu.edu.cn (Z.-h. Liu).

Nomenclature

$c_{p,1}$	specific heat (J/kg K)	Rq	standard roughness, $Rq = \sqrt{\frac{1}{L} \int_0^L Z(x)^2 dx}$
D	diameter of heat transfer surface (m)	Z	the ordinate of the profile curve
d	diameter of jet nozzle (m)	ΔT_{sat}	wall superheat (K)
G	mass flux of liquid jet (kg/m ² s)	ΔT_{sub}	subcooling of water (K)
h	heat transfer coefficient, (W/km ²)	v	impact velocity of jet flow at nozzle exit (m/s)
h_{fg}	latent heat of evaporation (J/kg)	x	axial position in the copper block (M)
L	the sampling length	Z	orthogonal position (M)
Nu	Nusselt number, $Nu = hd/\lambda$	λ	thermal conductivity (W/m ² K)
q	wall hat flux (W/m ²)	ν	kinematics viscosity (m ² /s)
$q_{c,0}$	CHF of saturated water (W/m ²)	σ	surface tension (N/m)
q_c	CHF of subcooled water (W/m ²)	ρ_l	liquid density (kg/m ³)
Pr	Prandtl number	ρ_v	vapor density (kg/m ³)
Re	Reynolds number, $Re = vd/\nu$		
Ra	Average roughness, $Ra = \frac{1}{L} \int_0^L Z(x) dx$		

understand the burnout phenomenon in nucleate boiling and represents the largest cooling capacity for the jet cooling. Many researchers have proposed a lot of semi-theoretical semi-empirical correlations for predicting the boiling heat transfer in nucleate and film boiling regimes, and the CHF for water jet impingement on conventional metal plates [4–17]. The geometries of a liquid jet impinging on a horizontal hot plate can be divided into two modes. One mode is the free surface jet, in which a large heated disk or rectangular plate is cooled by a small liquid jet and the ratio of the heated disk diameter to the nozzle diameter is much larger than unity. Another mode is the stagnation surface jet, in which the ratio of the heated disk diameter to the nozzle diameter is less than unity or equal to unity, and the heat transfer surface is in the jet stagnation zone. In the past two decades, for the free surface jet, the studies associated with the CHF of saturated and sub-cooled liquids on the conventional metal surface have been performed extensively. The typical empirical correlation was proposed by Monde [4] for predicting the CHF of saturated liquids as below,

$$\frac{q_{c0}}{GH_{\text{fg}}} = 0.0757 \left(\frac{\rho_v}{\rho_l} \right)^{0.275} \left(\frac{\sigma \rho_l}{G^2 d} \right)^{1/3} \frac{1}{1 + 0.00113(D/d)^2} \quad (1)$$

In the subsequent research, Monde [7] has proposed an empirical correlation for predicting the CHF of the sub-cooled liquids as below,

$$\frac{q_c}{q_{c0}} = \frac{1 + \sqrt{1 + 4CJa}}{2}$$

$$Ja = \left(\frac{\rho_l}{\rho_v} \right) \left(\frac{C_p \Delta T_{\text{sub}}}{H_{\text{fg}}} \right), \quad C = \frac{0.95(d/D)^2(1+D/d)^{0.364}}{(\rho_l/\rho_g)^{0.43}(2\sigma/\rho_l v^2(D-d))^{0.343}} \quad (2)$$

Up to now, the research about the free surface jet has confined to the conventional surface and has not considered the effect of the solid–liquid contact angle on the critical

heat flux. Only Liu [18] reported the effect of the superhydrophilic surface on the critical heat flux of jet boiling at a stagnation zone. The study on the effect of the solid–liquid contact angle on the jet boiling is very insufficient.

Take the previous studies into consideration; an experimental study was carried out to investigate jet boiling heat transfer characteristics on the superhydrophilic surface under the free surface condition in this study. The main interest was focused on the effect of the solid–liquid contact angle on the nucleate boiling and the CHF points. The boiling heat transfer and the CHF on the conventional copper surface, the TiO₂ coated surface and the superhydrophilic surfaces (TiO₂ coated surface under the exposure of ultra-violet light) were compared with each other. Three influencing parameters, subcooling, impact velocity and the contact angle, were changed and their effects on the nucleate boiling and the CHF were systemically studied. The empirical correlations were obtained for predicting the nucleate boiling heat transfer coefficient and the CHF on the superhydrophilic surface.

2. Coating process

The superhydrophilic surface was made by the dipping method in the coating process. In the dipping method, TiO₂ colloid was used. The specimen is a copper block. Prior to dipping, the specimen is cleaned and dried. The heat transfer surface was polished to mirror finish and washed by hydrochloric acid and then by the acetone and ion-exchanged water. When the surface becomes dry, the specimen is dipped into TiO₂ colloid then extracted slowly. After this dipping process, the specimen, hydrolyzed in the moist air for 24 h, is put into the muffle and heated to 450 °C by a heating velocity of 5 °C per minute. The specimen is heated for an hour in the muffle and allowed to cool slowly. The thickness of the coated layer was measured by an interferometer. The thickness was about 1 μm. The TiO₂ coated surface will produce superhydrophilic characteristic after being exposed to ultra-violet light gradually. After

2 h, the superhydrophilic characteristic remains stable and the surface wettability would not change any more.

The contact angle is measured by means of sessile drop method in room temperature. The specimen is irradiated with ultra-violet lights of the peak wavelengths between 275 nm and 315 nm. For the superhydrophilic surface, the water drop would entirely expand on the superhydrophilic surface and covered the whole surface. Therefore, the accurate value of the contact angle cannot be obtained. However, it can be confirmed that the contact angle on the superhydrophilic surface is close to zero. When there is no ultra-violet light, the contact angle on the TiO₂ coated surface is between 20° and 40°, while the contact angle on the copper surface is between 40° and 70°. Afterwards, the TiO₂ coated surface under the ultra-violet light is named as the superhydrophilic surface and the TiO₂ coated surface not exposed under the ultra-violet light is named as the TiO₂ coated surface.

The different ultra-violet luminous intensities were used for irradiating the TiO₂ coated surface. It is found that the luminous intensity has no effect on the contact angle. on the other hand, the effects of the thickness and non-uniformity of the TiO₂ coated layer on the wettability also have not been found in the prior test.

By making use of atomic force microscope, the surface roughness on the conventional copper surface and the TiO₂ coated surface can be measured. the pictures of surface roughness are shown in Fig. 1. In addition, the 2d and 3d microphotographs of the two surface states are also shown in Fig. 1.

As to the copper surface, the average surface roughness $Ra = 194.01$ nm and standard surface roughness $Rq = 254.93$ nm. However, for the TiO₂ coated surface, $Ra = 106.61$ nm and $Rq = 130.92$ nm. It is found that the roughness on the TiO₂ coated surface is significantly less than that on the copper surface.

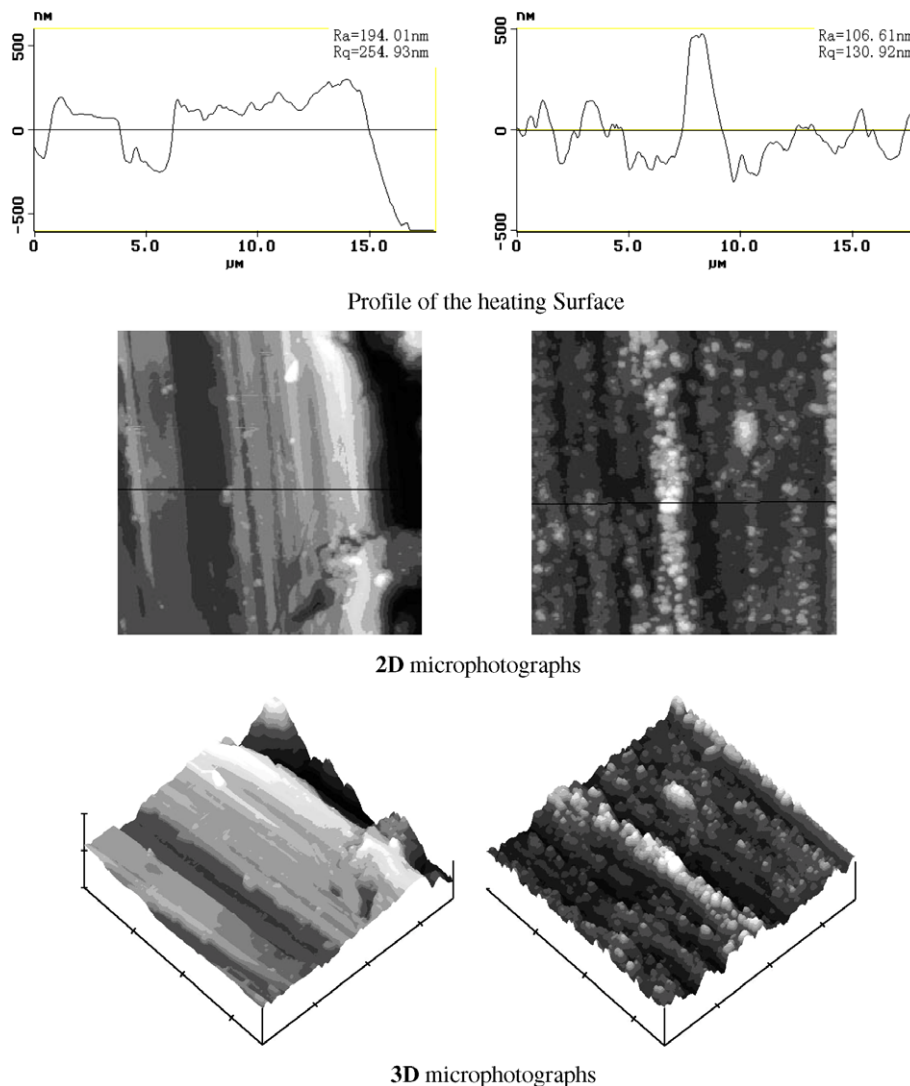


Fig. 1. Roughness profiles and microphotographs of the copper surface (left) and the TiO₂ coated surface (right).

3. Experimental procedure

Fig. 2 shows the schematic diagram of the experimental apparatus. It mainly consisted of the water tank, the test box, the circulation system of the test liquids, the measuring devices and the electric power supply. Fig. 3 shows the schematic diagram of the test box. Ion-exchanged water was used as the working liquid. Before the test run starting, the temperature of water was firstly increased to a set value by an auxiliary heater in the water tank and the coated surface was exposed to the ultra-violet light for 2 h. When the test run started, the water was drained from the water tank by a pump, passed through a regulating valve and a flow meter, flowed into the jet nozzle made of a quartz glass tube, in which the temperature of the water was finally measured by a thermocouple. The distance between the heat transfer surface and the nozzle was fixed at 5.0 mm. The heated block was a vertical copper bar having 50 mm diameter and 120 mm height, whose top surface was a smooth, horizontally circular heat transfer surface. The copper bar was heated with a ribbon electric heater (main heater), which was twisted outside of the copper bar. The superhydrophilic surface heat transfer surface was coated with TiO₂. The isinglass sheet was used as the insulator between the copper bar and the main heater.

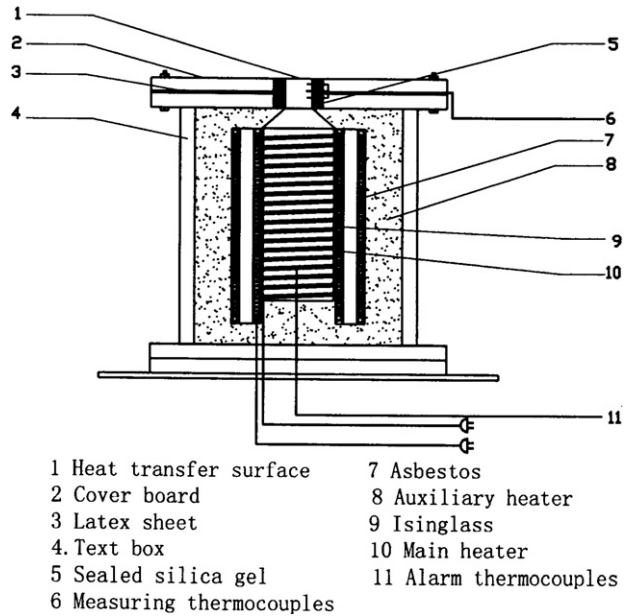


Fig. 3. Schematic diagram of test box.

The copper bar was placed in a thick ceramic tube; another ribbon electric heater (auxiliary heater) was twisted outside of the ceramic tube to prevent the heat losses from the cop-

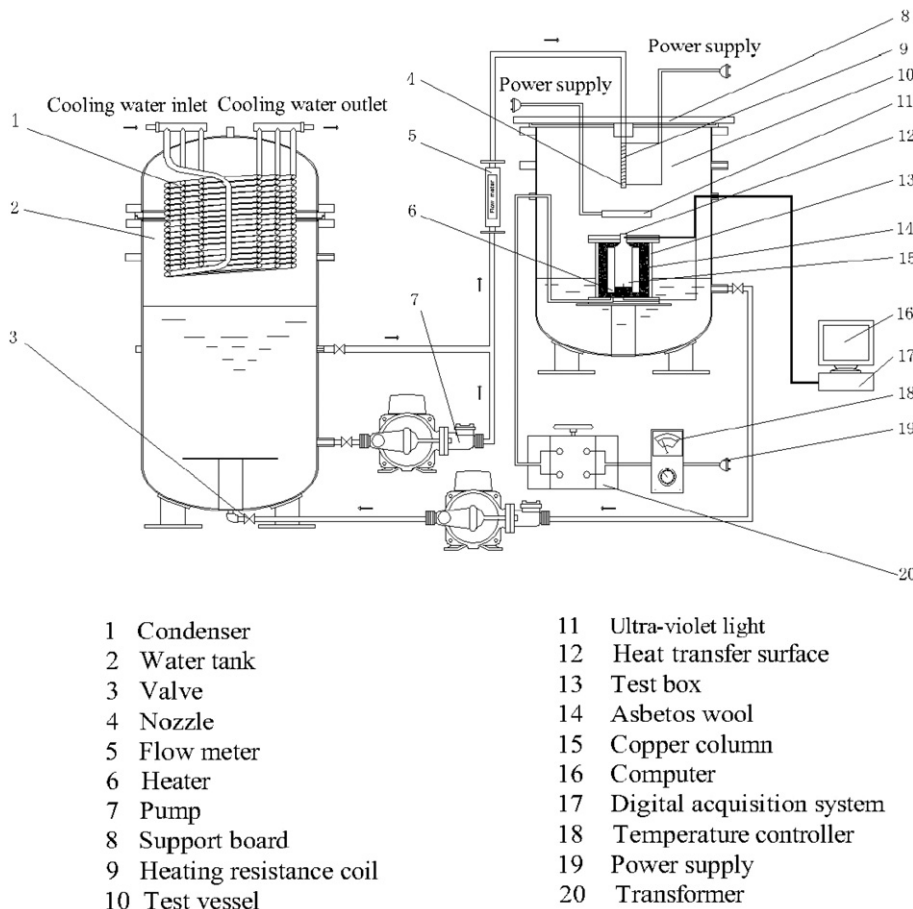


Fig. 2. Schematic diagram of the experimental apparatus.

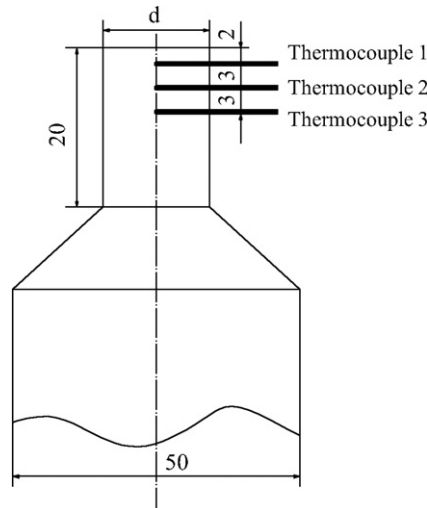


Fig. 4. Layout of measuring thermocouples in copper block (unit: mm).

per bar. Fig. 4 shows the layout of measuring thermocouples in the copper block. The horizontal heat transfer surface with diameter of 20 mm was used in this experiment. In the upper column of the copper bar, three 1.0 mm/ \varnothing thermocouples were horizontally inserted at the center axial line of the copper bar. The distances between the thermocouples were 3.0 mm and the distance between the top thermocouples and the heat transfer surface was 2.0 mm. Signals from the thermocouples mounted in the copper bar were measured by a digital voltmeter (Agilent-34950 A) and then fed into a computer, which converted them to the wall temperatures and wall fluxes by using a steady one-dimensional thermal conduction equation along the vertical direction. One of them was fed into a PID temperature controller as a feedback signal, which adjusted the power supply. In the tests, the electric power of the auxiliary heater was carefully adjusted to prevent the heat losses from the main heater. The test box, which was made of stainless steel, had a diameter of 250 mm and a height of 200 mm. The space inside the test box was filled by asbestos. All of the measurements were performed in the steady state, the temperatures and heat fluxes of the heat transfer surface were calculated from the temperature differences between two thermocouples mounted on the center axial line of the copper bar. A monitor thermocouple inserted at the bottom of the copper bar was connected to a temperature controller that prevents the maximum temperature of the copper bar from exceeding 750 °C. Our prepared experiment and other concerning studies have shown that the boiling heat transfer coefficients either in the stagnation zone or in the free flow zone were the same for a jet boiling. Therefore, the boiling heat transfer characteristics on the whole heat transfer surface can be represented by that on the stagnation point. In the present experiment, three thermocouples were mounted on the upper column of the copper bar, as shown in Fig. 3. The temperature distributions showed very well linear relationship. Therefore, the one-

Table 1

Experimental conditions

Experimental parameters	Value of parameters
Test liquid	Ion-changed water
Reynolds number of jet flow (Re)	2.5×10^4 – 4×10^5
Heating condition	Steady
Wavelength of ultra-violet light	275–315 nm
Test pressure	Atmospheric pressure
Jet impact velocity, v (m/s)	0.5–6.5
Diameter of nozzle, d (mm)	4
Diameter of heat transfer surface, D (mm)	20
Subcooling, ΔT_{sub} (K)	0–74

dimensional heat conduction in the vertical direction satisfied in the upper column of the copper. Furthermore, the numerical simulation that has been carried out by previous researchers has also verified this conclusion.

During each run, electric power was increased gradually. The computer not only measured the wall temperature and wall heat flux instantaneously, but also gave an alarm when the wall temperature increased quickly and did not attain a steady state. Such an alarm means that the boiling crisis has occurred; therefore, the electric power was automatically cut off. After the boiling crisis occurred, the test was repeated from the steady state of the former time, the output electric power increased slowly by an increment of 1% of the electric power of the former time. When the boiling crisis occurred again, the test was stopped and the wall heat flux of the former time was determined as the CHF.

Table 1 shows the experimental conditions. In this experiment, the impact velocity ranged from 0.5 to 6.5 m/s, and, the wave of the impact velocity was limited within $\pm 4\%$. The diameter of the heat transfer surface was 20 mm, and the diameter of jet nozzle was 4 mm, respectively. The calibration errors of the thermocouples were less than 0.2 K. The maximum location deviation between thermocouples was about 0.01 mm. The maximum deviation of calculated thermal conductivity was estimated as 2%. The maximum uncertainties of the wall superheat and wall heat flux were about 4% and 6%.

4. Results and discussion

Figs. 5 and 6 show respectively the experimental data of the nucleate boiling regime for the saturated water and the subcooled water jet impingement on the superhydrophilic surface for the impact velocity ranging from 1 to 6 m/s. As a comparison, the empirical correlation by Wolf et al. [10] for predicting the jet boiling heat transfer of water on a stainless steel surface was also shown in Figs. 5 and 6.

$$q = 63.7 \Delta T_{\text{sat}}^{2.9} [\text{W/m}^2 \text{K}] \quad (3)$$

The jet boiling experiment of water on the copper surface was also carried out in the present study. The experimental data agreed reasonably well with Eq. (3). Therefore, in Figs. 5 and 6, the calculated values from Eq. (3) may denote the jet boiling heat transfer on the copper surface.

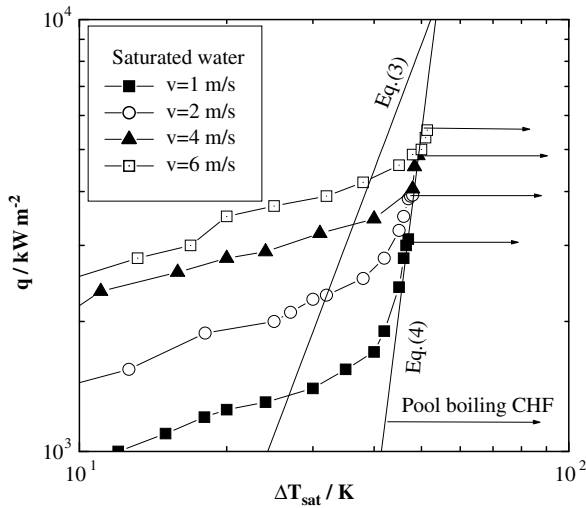


Fig. 5. Boiling curves of saturated water jet on the superhydrophilic surface with different velocity.

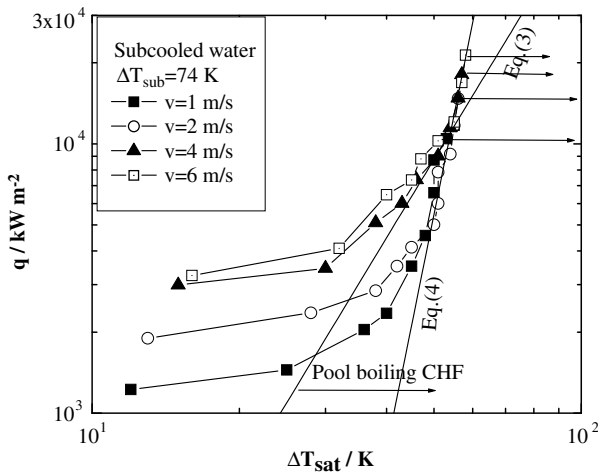


Fig. 6. Boiling curves of subcooled water jet on the superhydrophilic surface with different velocity.

It is found that the nucleate boiling incipience on the superhydrophilic surface is greatly delayed. The experimental range mainly belongs to the forced convective regime. In the fully developed nucleate boiling regime, the boiling curves are quite steep. To each velocity, the superheat corresponding to the CHF lies in a narrow range from 50 to 55 K. The boiling curves resulted from the different velocities essentially converge into a steep line. The superhydrophilic surface plays an important role to the jet boiling heat transfer characteristics.

In the author’s previous study [18], which experimentally investigated the nucleate boiling heat transfer characteristics of a round water jet impingement in a flat stagnation zone with the same size as the jet nozzle on the superhydrophilic surface, the following empirical correlation was proposed and it could well predict the nucleate boiling heat transfer of water jet on a superhydrophilic surface on a stagnation zone.

$$q = 2.8 \times 10^{-9} \times \Delta T_{\text{sat}}^9 \quad (4)$$

The present experimental data from the free surface jet system which has a small jet nozzle and a large heat transfer surface still can agree well with the predictions of Eq. (4) within the relative errors of $\pm 6\%$. Therefore, it is confirmed that the formation of jet (free surface jet or stagnation zone jet) has no any effect on the nucleate boiling characteristics on the superhydrophilic surface.

Fig. 7 shows the compared results of the CHF data of the saturated water jet boiling among the superhydrophilic surface, the TiO₂ coated surface and the copper surface. According to the Eq. (1), we have known that there exists a function relation between $q_{c,0}$ and v for the saturated water jet on the conventional metal surface. No matter for the superhydrophilic surface or for the TiO₂ coated surface, it is found that there still exists a same relation between the CHF and v as for the conventional metal surface. Therefore, the form of Eq. (1) is still available for the superhydrophilic surfaces. The difference is that the CHF on superhydrophilic surface is about 30% higher than that on the conventional metal surface. Therefore, for the superhydrophilic surfaces, using a least square fit within the relative errors of $\pm 5\%$, the CHF predicting correlation can be presented as the follow.

$$\frac{q_{c0}}{GH_{\text{fig}}} = 0.0985 \left(\frac{\rho_v}{\rho_l} \right)^{0.275} \left(\frac{\sigma \rho_l}{G^2 d} \right)^{1/3} \frac{1}{1 + 0.00113(D/d)^2} \quad (5)$$

Fig. 8 shows the experimental data of the CHF for subcooled water jet impingement on the superhydrophilic and copper surfaces with different velocities. Similar to the case for the saturated water jet boiling, for the subcooled water jet boiling, there still exists a good proportional relation between the CHF of the superhydrophilic and copper surfaced. The CHF on the superhydrophilic surface is about 30% higher than that on conventional metal surface for the different velocities and subcooling in the

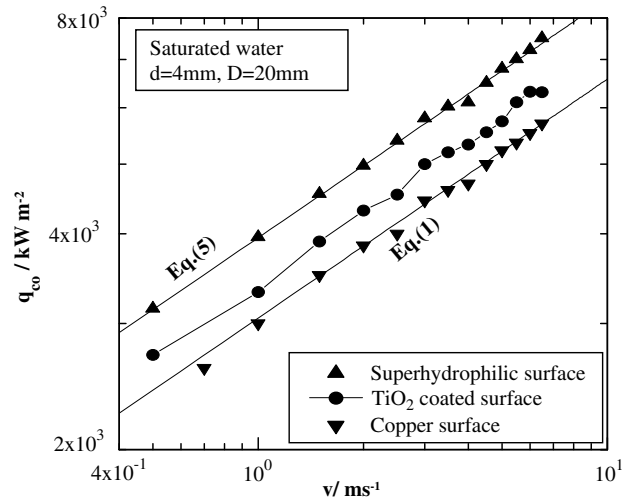


Fig. 7. The CHF of saturated water jet impingement on superhydrophilic surface with different velocities.

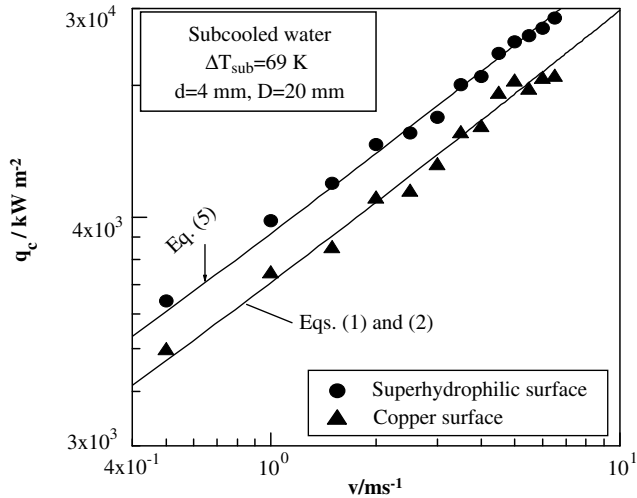


Fig. 8. The CHF of subcooled water jet impingement on superhydrophilic surface with different velocities.

test range. Therefore, the effects of the superhydrophilic surface on the CHF are the same either for saturated water or for the subcooled water.

Fig. 9 shows the comparison of the CHF data of the subcooled water jet on the superhydrophilic surface with Eq. (2) for different subcoolings. Here, the q_c and $q_{c,0}$ respectively denote the CHFs of the subcooled water and the saturated water on the superhydrophilic surface. Eq. (2) correlates the CHF data with the maximum relative errors less than 5%, and can still be used for predicting the CHF of the subcooled water jet boiling on the superhydrophilic surface. Since the CHF on the superhydrophilic surface increases 30% than that on the copper surface either for saturated water or for the subcooled water at the fixed flow parameters, Eq. (2) can be naturally employed for predicting the CHF on the superhydrophilic surface.

For a stagnation zone jet, the CHF on the superhydrophilic surface is about 50% higher than that on common

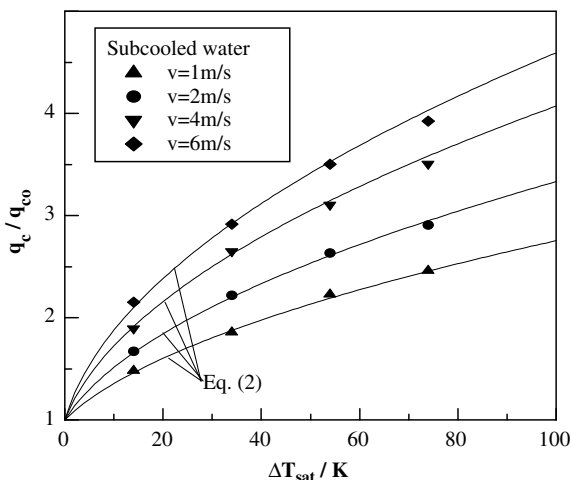


Fig. 9. The effect of subcooling to the CHF on the superhydrophilic surface.

copper surface [8]. It is confirmed that the formation of jet has great effect on the increase of the CHF. The reason should be from difference of the flow construction.

To the pool boiling, it has been well known that the CHF is increasing with the decreasing of the solid–liquid contact angle. The mechanism has been theoretically discovered by many researchers [19–21]. But to jet boiling, the relationship between the contact angle and the CHF may be more complicated than that of pool boiling. We suggest that for the superhydrophilic surface, as in the pool boiling, the infiltration capability toward the liquid subfilm on the heat transfer surface is increasing. Therefore, the great CHF is needed for occurring boiling crisis.

The solid–liquid contact angle is the function of both the physical properties of the solid surface and the working liquid. Almost all of the researchers carried out the various jet boiling experiments by making use of conventional metal heat transfer surface such as copper, stainless steel etc. Therefore, for the conventional metal surface, the solid surface physical properties are basically constant, and the contact angle mainly depends on the physical properties of working liquids. Namely, the magnitude of contact angle can be represented as a function of the surface tension of liquids. The effect of the different contact angle between the high wettability liquids and weak wettability liquids on the CHF may be represented as the effect of the surface tension. However, for the superhydrophilic surface, the contact angle not only depends on the liquid physical properties, but also depends on the surface physical properties. Therefore, the contact angle is a special parameter. Its effect cannot be included only in the effect of surface tension. To understand the combined effects of both the surface physical properties of solid surface and working liquids, a lot of further work is needed.

5. Conclusions

An experimental investigation was carried out for predicting CHF of a bar water jet impingement on a large flat superhydrophilic surface. The following conclusions were obtained.

1. The superhydrophilic surface can significantly increase the CHF of water jet boiling on a flat heat transfer surface under the free surface jet condition., because it remarkably decreasing the solid–liquid contact angle.
2. The superhydrophilic surface delays greatly boiling incipience and worsen the boiling heat transfer in the fully developed nucleate boiling regime.
3. The qualitative effects of the impact velocity and the subcooling of water on the CHF for the superhydrophilic surface are the same as that for the conventional copper surface. However, the CHF on the superhydrophilic surface is about 30% higher than that on conventional copper surface.
4. The empirical correlations (4) and (5) are obtained for predicting the fully developed boiling heat transfer and

the CHF of steady boiling for the saturated and subcooled water jet impingement on the flat superhydrophilic surface.

Acknowledgement

This work was supported by the national natural science foundation of China under Grant No. 50176029.

References

- [1] R. Wang, K. Hashimoto, A. Fujishima, M. Chikuni, E. Kojima, A. Kitamura, M. Shimohigoshi, A. Watanabe, Light-induced amphiphilic surfaces, *Nature* 388 (1997) 431–432.
- [2] Y. Takata, S. Hidaka, J.M. Cao, K. Tanaka, M. Masuda, T. Ito, T. Watanabe, M. Shimohigoshi, Boiling and evaporation from a superhydrophilic surface, *Therm. Sci. Eng.* 8 (2000) 33–41.
- [3] Y. Takata, S. Hidaka, J.M. Cao, T. Nakamura, H. Yamamoto, M. Masuda, T. Ito, Effect of surface wettability on boiling and evaporation, *Energy* 30 (2005) 209–220.
- [4] M. Monde, Burnout heat flux in saturated forced convection boiling with an impinging jet, *Heat Transfer Jap. Res.* 9 (1980) 31–41.
- [5] C.F. Ma, A.E. Bergles, Jet impinging nucleate boiling, *Int. J. Heat Mass Transfer* 29 (1986) 1095–1101.
- [6] Y. Katto, S. Yokoya, Critical heat flux on a disk heater cooling by a circular jet of saturated liquid impinging at the center, *Int. J. Heat Mass Transfer* 31 (1988) 219–227.
- [7] M. Monde, K. Kitajima, T. Inoue, Y. Mitsutake, Critical heat flux in a forced convective subcooled boiling with an impinging jet, *ASME, J. Heat Transfer* 7 (1994) 515–520.
- [8] S. Kumagai, T. Sano, T. Kamata, S. Suzuki, R. Kubo, Boiling heat transfer to an impinging jet in cooling a hot metal slab, *Trans. JSME (B)* 60 (1994) 259–263.
- [9] M. Monde, Y. Mitsutake, Critical heat flux in a convection subcooled boiling with multiple impinging jets, *ASME, J. Heat Transfer* 117 (1996) 241–243.
- [10] D.H. Wolf, F.P. Incropera, R. Viskanta, Local jet impingement boiling heat transfer, *Int. J. Heat Mass Transfer* 39 (1996) 1395–1406.
- [11] Z.H. Liu, J. Wang, Study on film boiling heat transfer for water jet impinging on a high temperature flat plate, *Int. J. Heat Mass Transfer* 44 (2001) 2475–2481.
- [12] H. Robidou, H. Auracher, P. Gardin, M. Lebouche, Controlled cooling of a hot plate with a water jet, *Exp. Therm. Fluid Sci.* 26 (2002) 123–129.
- [13] Z.H. Liu, Q.Z. Zhu, Predication of critical heat flux for convective boiling of saturated water jet impingement on the stagnation zone, *ASME, J. Heat Transfer* 124 (2002) 1125–1130.
- [14] Z.H. Liu, Prediction of minimum heat flux for water jet boiling on a hot plate, *J. Thermophys. Heat Transfer* 17 (2003) 159–16516.
- [15] Y.H. Qiu, Z.H. Liu, Critical heat flux in saturated and subcooled boiling for R-113 jet impingement on the stagnation zone, *Appl. Therm. Eng.* 25 (2005) 2367–2378.
- [16] Z.H. Liu, T.F. Tong, Y.H. Qiu, Critical heat flux of steady boiling for subcooling water jet impingement on the flat stagnation zone, *ASME J. Heat Transfer* 126 (2004) 179–183.
- [17] Y.H. Qiu, Z.H. Liu, Critical heat flux of steady boiling for saturated liquids jet impinging on the stagnation zone, *Int. J. Heat Mass Transfer* 48 (2005) 4590–4597.
- [18] Z.H. Liu, Y.H. Qiu, Critical heat flux of steady boiling for water jet impingement in flat stagnation zone on superhydrophilic surface, *ASME, J. Heat Transfer* 128 (7) (2006) 726–729.
- [19] K. Sefiane, D. Benielli, A. Steinchen, A new mechanism for pool boiling crisis. Recoil instability and contact angle influence, *Coll. Surf.* 142 (1998) 361–373.
- [20] J.H. Sang, C.N. Hee, A dry-out model of critical heat flux applicable to both pool boiling and subcooled forced convection boiling, *Int. J. Heat Mass Transfer* 43 (2000) 241–250.
- [21] A.G. Kandlikar, A theoretical model to predict pool boiling CHF incorporating effects of contact angle and orientation, *ASME, J. Heat Transfer* (2001), pp. 123, 1071–1078.